

# $\Lambda$ and $\bar{\Lambda}$ polarization from deep inelastic muon scattering

E665 Collaboration

M.R. Adams<sup>6</sup>, M. Aderholz<sup>12</sup>, S. Aid<sup>10</sup>, P.L. Anthony<sup>9</sup>, D. Ashery<sup>2,18</sup>, D.A. Averill<sup>6</sup>, M.D. Baker<sup>11</sup>, B.R. Baller<sup>4</sup>, A. Banerjee<sup>15</sup>, A.A. Bhatti<sup>16</sup>, U. Bratzler<sup>16</sup>, H.M. Braun<sup>17</sup>, T.J. Carroll<sup>12</sup>, H.L. Clark<sup>14</sup>, J.M. Conrad<sup>5</sup>, R. Davison<sup>16</sup>, I. Derado<sup>12</sup>, F.S. Dietrich<sup>9</sup>, W. Dougherty<sup>16</sup>, T. Dreyer<sup>1</sup>, V. Eckardt<sup>12</sup>, U. Ecker<sup>17</sup>, M. Erdmann<sup>1</sup>, G.Y. Fang<sup>5</sup>, J. Figiel<sup>8</sup>, R.W. Finlay<sup>14</sup>, H.J. Gebauer<sup>12</sup>, D.F. Geesaman<sup>2</sup>, K.A. Griffioen<sup>15</sup>, R.S. Guo<sup>6</sup>, J. Haas<sup>1</sup>, C. Halliwell<sup>6</sup>, D. Hantke<sup>12</sup>, K.H. Hicks<sup>14</sup>, H.E. Jackson<sup>2</sup>, G. Jancso<sup>7</sup>, D.M. Jansen<sup>16</sup>, Z. Jin<sup>16</sup>, K. Kadija<sup>12</sup>, S. Kaufmann<sup>2</sup>, R.D. Kennedy<sup>3</sup>, E.R. Kinney<sup>2</sup>, H.G.E. Kobrak<sup>3</sup>, A.V. Kotwal<sup>5</sup>, S. Kunori<sup>10</sup>, M. Lenski<sup>1</sup>, J.J. Lord<sup>16</sup>, H.J. Lubatti<sup>16</sup>, D. McLeod<sup>6</sup>, A. Manz<sup>12</sup>, H. Melanson<sup>4</sup>, D.G. Michael<sup>5</sup>, H.E. Montgomery<sup>4</sup>, J.G. Morfin<sup>4</sup>, R.B. Nickerson<sup>5</sup>, K. Olkiewicz<sup>8</sup>, L. Osborne<sup>11</sup>, R. Otten<sup>17</sup>, V. Papavassiliou<sup>2</sup>, B. Pawlik<sup>8</sup>, F.M. Pipkin<sup>†5</sup>, D.H. Potterveld<sup>2</sup>, A. Röser<sup>17</sup>, J.J. Ryan<sup>11</sup>, C.W. Salgado<sup>4</sup>, H. Schellman<sup>13</sup>, M. Schmitt<sup>5</sup>, N. Schmitz<sup>12</sup>, G. Siegert<sup>1</sup>, A. Skuja<sup>10</sup>, G.A. Snow<sup>10</sup>, S. Söldner-Rembold<sup>12</sup>, P. Spentzouris<sup>4</sup>, P. Stopa<sup>8</sup>, R.A. Swanson<sup>3</sup>, V. Topor Pop<sup>18</sup>, H. Venkataramania<sup>13</sup>, M. Wilhelm<sup>1</sup>, Richard Wilson<sup>5</sup>, W. Wittek<sup>12</sup>, S.A. Wolbers<sup>4</sup>, A. Zghiche<sup>2</sup>, T. Zhao<sup>16</sup>

<sup>1</sup>Albert-Ludwigs-Universität Freiburg i. Br., Germany

<sup>2</sup>Argonne National Laboratory, Argonne, Illinois 60439

<sup>3</sup>University of California, San Diego, California 92093

<sup>4</sup>Fermi National Accelerator Laboratory, Batavia, Illinois 60510

<sup>5</sup>Harvard University, Cambridge, Massachusetts 02138

<sup>6</sup>University of Illinois, Chicago, Illinois 60680

<sup>7</sup>KFKI Research Institute for Particle and Nuclear Physics, H-1525 Budapest, Hungary

<sup>8</sup>Institute for Nuclear Physics, Krakow, Poland

<sup>9</sup>Lawrence Livermore National Laboratory, Livermore, California 94551

<sup>10</sup>University of Maryland, College Park, Maryland 20742

<sup>11</sup>Massachusetts Institute of Technology, Cambridge, Massachusetts 02139

<sup>12</sup>Max-Planck-Institut für Physik, Munich, Germany

<sup>13</sup>Northwestern University, Evanston, Illinois 60208

<sup>14</sup>Ohio University, Athens, Ohio 45701

<sup>15</sup>University of Pennsylvania, Philadelphia, Pennsylvania 19104

<sup>16</sup>University of Washington, Seattle, Washington 98195

<sup>17</sup>University of Wuppertal, Wuppertal, Germany

<sup>18</sup>Tel Aviv University, Tel Aviv, Israel

† deceased

## Abstract

We report results of the first measurements of  $\Lambda$  and  $\bar{\Lambda}$  polarization produced in deep inelastic polarized muon scattering on the nucleon. The results are consistent with an expected trend towards positive polarization with increasing  $x_F$ . The polarizations of  $\Lambda$  and  $\bar{\Lambda}$  appear to have opposite signs. A large negative polarization for  $\Lambda$  at low positive  $x_F$  is observed and is not explained by existing models. A possible interpretation is presented.

The spin structure function of the nucleon has been studied extensively during the past several years. Very different experimental systems utilizing polarized muon [1], electron [2] and positron [3] beams and covering different kinematic regions obtained results which are consistent with each other. This effort led to precise measurements of the nucleon spin structure functions  $g_1^N(x)$  ( $N = n, p$ ) and their integrals  $\Gamma_1^N = \int g_1^N(x) dx$ . Here  $x \equiv x_{Bj} = Q^2/2M\nu$  is the Bjorken scaling variable,  $-Q^2$  is the four-momentum transfer to the target nucleon squared,  $\nu$  is the energy loss of the lepton in the laboratory frame, and  $M$  is the nucleon mass. The interpretation of these results is that quarks in the nucleon carry only  $\sim 30\%$  of the nucleon spin and that the strange (and non-strange) sea is polarized opposite to the polarization of the valence quarks. This interpretation leads to the question of where the rest of the nucleon spin is coming from which will not be addressed here. Other open questions are: 1) how sensitive are the conclusions to the SU(3) flavor symmetry assumed in the interpretation of the experimental data? 2) what is the mechanism that polarizes the strange sea? 3) how well do we understand the spin structure of other hadrons? 4) are the quarks and antiquarks in the sea equally polarized?

We have addressed these questions with a measurement of the polarization of  $\Lambda$  and  $\bar{\Lambda}$  hyperons produced in polarized muon Deep Inelastic Scattering (DIS) on unpolarized targets. Having the strange quark as valence rather than sea quark, the polarization of  $\Lambda$  hyperons is sensitive to its contribution to the  $\Lambda$  spin. By measuring both  $\Lambda$  and  $\bar{\Lambda}$  polarization the roles of both  $s$  and  $\bar{s}$  can be studied. Models exist that describe mechanisms of the strange sea polarization [4, 5] and predict the  $\Lambda$  polarization in the target fragmentation region. Other models are based on the naïve quark model or invoke SU(3) symmetry to calculate the spin structure function of the  $\Lambda$  from that of the nucleon [6, 7, 8, 9, 10, 11]. These models predict the  $\Lambda$  and  $\bar{\Lambda}$  polarization in the current fragmentation region. These predictions can be tested by measuring the polarization of the  $\Lambda$  and  $\bar{\Lambda}$ .

As an illustration, a simple mechanism that can produce  $\Lambda$  polarization in polarized lepton DIS is the following: the polarized virtual photon is absorbed by a strange quark in the target nucleon sea. The struck quark then emerges with spin aligned in the direction of that of the photon. When it hadronizes into a  $\Lambda$  (in the current fragmentation region), it is likely to become a valence quark in the  $\Lambda$  and the naïve quark model predicts that the polarization of the  $\Lambda$  will be the same as that of the strange quark. An experiment that can probe the low  $x_{Bj}$  region will have a significant fraction of the  $\Lambda$  and  $\bar{\Lambda}$  originating from this mechanism and will therefore have sensitivity to the strange sea in the target nucleon. When the DIS kinematics selects the sea quarks (low  $x_{Bj}$ ) the probability that the struck quark will be a strange quark is about an order of magnitude smaller than for it to be a  $u$  or  $d$  quark. This is because the scattering probability is proportional to the electric charge squared and there are half as many strange quarks in the sea as there are  $u$  and  $d$  quarks. However, if  $u$  or  $d$  quarks are struck out their probability to hadronize into a strange baryon is small [12]. On the other hand, if a strange quark is struck out it will *always* hadronize into a strange particle including baryons. It can therefore be expected that a significant fraction of leading strange baryons will carry the strange struck quark.

The transfer of polarization from the beam to the produced  $\Lambda$  and  $\bar{\Lambda}$  is controlled by their helicity difference fragmentation functions  $\Delta\hat{q}_\Lambda$ . 'Complexities' in the analysis of fragment polarization, as defined in reference [8], are proportional to  $\sin^2\theta_\mu$  where  $\theta_\mu$  is the laboratory scattering angle of the muon. If these are small, as they are in this experiment, the measured polarization of a  $\Lambda$  produced in DIS of muons having polarization  $P_\mu$  is given by:

$$\vec{P}_\Lambda^{meas} = \vec{P}_\mu D(y) \frac{\sum_q e_q^2 q_N(x, Q^2) \Delta\hat{q}_\Lambda(z, Q^2)}{\sum_q e_q^2 q_N(x, Q^2) \hat{q}_\Lambda(z, Q^2)}. \quad (1)$$

Here  $D(y) = y(2 - y)/[1 + (1 - y)^2]$ ,  $y = \nu/E_\mu$ ,  $e_q$  and  $q_N$  are the charge and  $x$ -distribution of the quark with flavor  $q$ , respectively, and  $z$  is the energy of the produced hadron divided by  $\nu$ . In recent measurements at LEP  $\Delta\hat{q}$  was measured from  $\Lambda$  polarization near the  $Z$  pole and was found to be consistent with the naïve quark model expectations [13, 14].

In this paper we present the first results of  $\Lambda$  and  $\bar{\Lambda}$  polarization measured in DIS with polarized muon beams. These results were obtained from data taken by the Fermilab E665 collaboration. In the experiment a 470 GeV/c positive muon beam was scattered off hydrogen, deuterium and several nuclear targets. The scattered muons and the final state hadrons were reconstructed in an open-geometry double-dipole spectrometer which had acceptance for forward produced charged hadrons. A more complete description of the experimental system can be found elsewhere [15]. The muon beam, which comes from  $\pi$  and  $K$  decays is naturally polarized at a level determined by the beam optics. The polarization of the muon beam was calculated to be  $P_\mu = -0.7 \pm 0.1$ . The analysis presented here covers  $10^{-4} < x_{Bj} < 10^{-1}$  with  $\langle x_{Bj} \rangle = 5 \cdot 10^{-3}$ ,  $0.25 < Q^2 < 2.5 \text{ GeV}^2/c^2$  with  $\langle Q^2 \rangle = 1.3 \text{ GeV}^2/c^2$  and  $\langle \nu \rangle = 150 \text{ GeV}$ . The values of  $\sin^2\theta_\mu$  are less than  $10^{-4}$  which satisfies the above mentioned conditions. The data was taken with unpolarized hydrogen and deuterium targets.

The  $\Lambda$  and  $\bar{\Lambda}$  were identified by applying a kinematic fit to pairs of a positive and a negative track and reconstructing their invariant mass. The fit exploited the different kinematics that characterize the  $\Lambda \rightarrow \pi p$  and  $K^0 \rightarrow \pi^+\pi^-$  decays and selected events likely to be the former. This and the requirement that the decay vertex is downstream, well separated from the production vertex and pointing to it led to the selection of a very clean signal. Background effects were studied by varying the  $\Lambda$  and  $\bar{\Lambda}$  selection criteria, in particular, by replacing the kinematic fit by other requirements such as inconsistency with the  $K^0$  mass if both tracks are assigned the pion mass. These criteria selected signals which left some background below and above the  $\Lambda$  mass peak. Using these two signals, and after subtracting the distributions of the background, we produced two  $\cos\theta_{p,\gamma^*}$  distributions as used to deduce the polarization (see below). The two distributions were found to be consistent with each other. Contributions of the background to the systematic uncertainties in the polarization were taken from comparison of these distributions. Secondary interactions were found to account for less than 3% of the events.

For the final sample we also required:  $m_{e^+e^-} > 0.05 \text{ GeV}$ ,  $\nu > 50 \text{ GeV}$ ,  $0.1 < y < 0.8$  and  $p_\pi > 4 \text{ GeV}/c$ . Here  $m_{e^+e^-}$  is the invariant mass of the track pair assuming that both tracks are electrons and  $p_\pi$  is the pion momentum. The size of the sample with the final cuts was about 750  $\Lambda$  and 650  $\bar{\Lambda}$  hyperons. The similarity of the  $\Lambda$  and  $\bar{\Lambda}$  yields is an important feature of this experiment and results from the low  $x_{Bj}$  sensitivity probing mainly the sea quarks of the target nucleon. The small difference may be caused by  $\Lambda$  hyperons produced by contribution from valence quarks in this  $x_{Bj}$  region. The size of the sample does not allow a detailed study of the  $x_F$  dependence of the polarization ( $x_F = p_l/p_{l \text{ max}}$  is the Feynman-x variable,  $p_l$  is the longitudinal momentum relative to the virtual-photon direction and  $p_{l \text{ max}}$  is the maximal value it can have, both in the hadronic c.m. system). We divided the sample into two  $x_F$  bins:  $0 < x_F < 0.3$  with  $\langle x_F \rangle = 0.15$  and  $0.3 < x_F < 1.0$  with  $\langle x_F \rangle = 0.44$ . We also present results for  $x_F > 0.1$ .

The angular distribution  $\theta_{p,\gamma^*}$  of the proton in the  $\Lambda \rightarrow \pi p$  decay is computed in the  $\Lambda$  rest frame with respect to the direction of the absorbed virtual photon. The measured angular distribution is shown in figure 1(a). This decay angular distribution is affected by detector acceptance. In order to correct for that we carried out extensive Monte Carlo simulations of the decay distributions applying the same analysis cuts as for the data. The primary  $\mu p$  interaction is simulated using the standard LUND event generator (LEPTO 5.2, JETSET 6.3 [16]). Initial and final state radiative events are generated with the GAMRAD [17] Monte Carlo. Particles produced at the interaction

vertex are tracked through the E665 spectrometer [15] using the GEANT [18] program. A detailed description of the Monte Carlo simulation has been documented elsewhere [19]. These simulations were found to reproduce well the distributions of many observables in this experiment and in the present analysis. In particular, good reproduction of the pion momentum distribution, a crucial parameter in this analysis, was observed for  $p_\pi > 3$  GeV/c.

The acceptance corrections were taken as the ratio of the number of generated events and the number of reconstructed events accepted by the selection criteria as applied to the data. In order to test possible background effects on these corrections we used two separate Monte Carlo simulations, one in which the ratio of generated  $K^0/\Lambda$  was about 12 and another in which it was about 0.6. In spite of the factor 20 difference in the ratio the two simulations yielded the same correction factors. The comparison was used to estimate the contribution from background in the simulations to the systematic uncertainties in the acceptance corrections. The acceptance-corrected angular distributions are expected to have the form:

$$I(\theta) = 1 + \alpha P_\Lambda^{meas} \cos \theta_{p,\gamma^*} \quad (2)$$

where  $P_\Lambda^{meas}$  is the measured  $\Lambda$  polarization and the value of the asymmetry parameter  $\alpha$  has been determined experimentally [20] to be  $0.642 \pm 0.013$  ( $-0.642$  for  $\bar{\Lambda}$ ). The experimental resolution in  $\cos \theta_{p,\gamma^*}$  was found to be about 0.02, small compared with the bin size. The acceptance-corrected angular distributions were fitted to straight lines. Such a distribution is shown in figure 1(b). We deduce the polarization of the  $\Lambda$  and  $\bar{\Lambda}$  from the slopes of the fits. After obtaining the polarizations we repeated the Monte Carlo simulations, this time introducing the measured polarization in the Monte Carlo generated events. After analysing the reconstructed events from the polarized Monte Carlo in the same way as the data the resulting distributions agreed well with those of the data (fig. 1(a)).

The systematic uncertainties in the results are due to uncertainties in the *slopes* of the acceptance corrections (not the absolute corrections). These were estimated from comparison of the slopes using the different selection criteria and using the various simulations: with different  $K^0/\Lambda$  ratios and with polarized and unpolarized generated distributions. The contributions from these sources were added in quadrature and resulted in a systematic uncertainty in the polarization of  $\pm 0.1$ , for both  $x_F$  bins.

In this analysis  $\cos \theta_{p,\gamma^*}$  is measured with respect to the virtual photon momentum. However, the interesting reference direction is that of the virtual photon spin. Since in this experiment the polarization of the muon beam and hence that of the virtual photon are negative we apply a minus sign to the results of the preceding analysis. The resulting measured polarizations are summarized in table 1. The total error  $\Delta P_\Lambda^{meas}$  is obtained by adding the systematic and statistical errors in quadrature. Finally, by dividing-out the diluting effects of the beam polarization  $|P_\mu| = 0.7 \pm 0.1$  and the photon depolarization factor  $D(y)$  which lies in the range 0.4 to 0.5, we obtain the undiluted polarizations  $P_\Lambda$  which are listed in table 1.

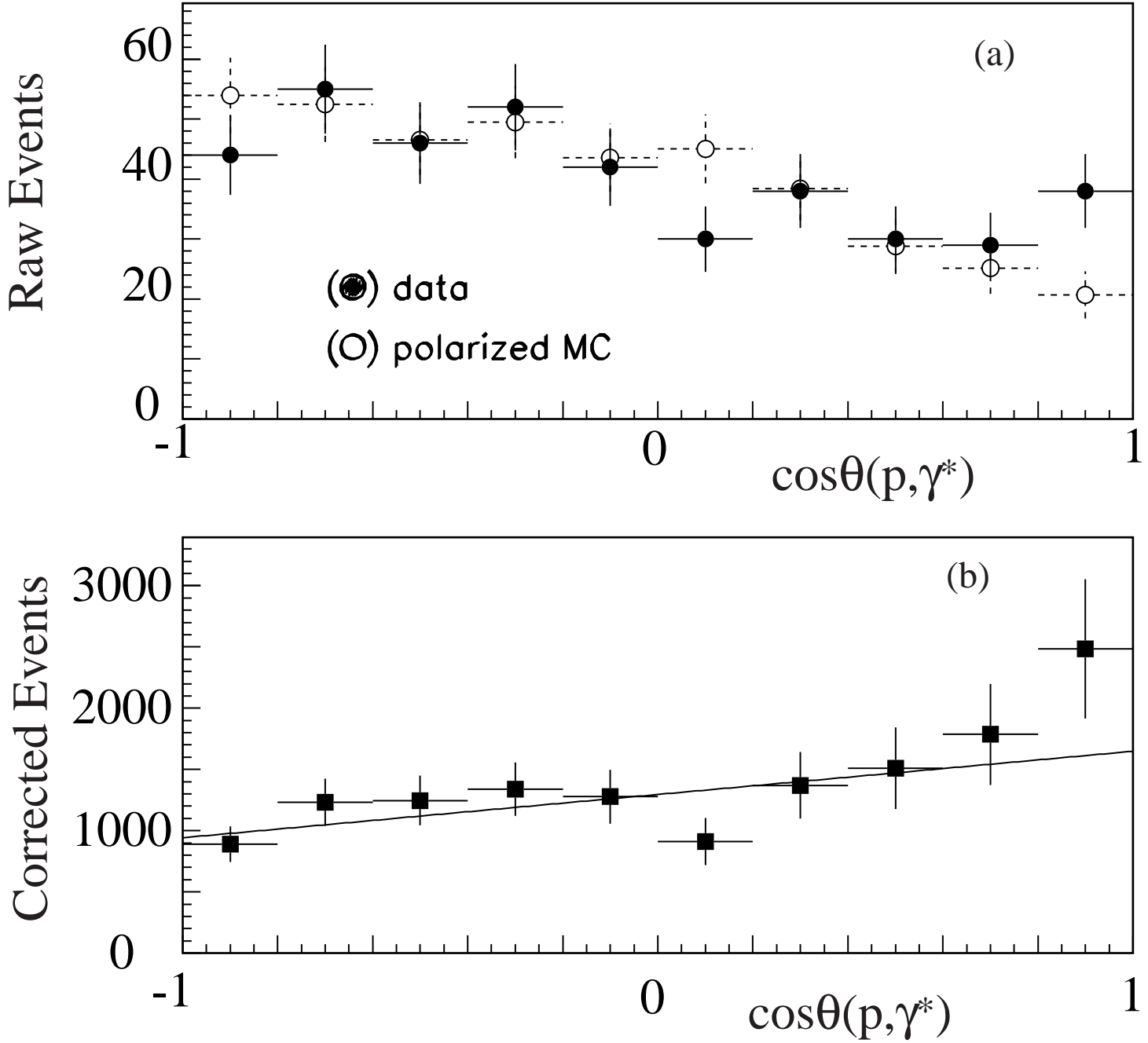


Figure 1:  $\cos\theta_{p,\gamma^*}$  distributions for  $\Lambda$  in the  $0 < x_F < 0.3$  region. (a) Raw data distribution and distribution of the polarized Monte Carlo simulation (see text). (b) Data corrected for experimental acceptance and the linear fit ( $\chi^2/dof = 1.2$ ) used to deduce the polarization. Shown are statistical errors only.

In the present analysis we cannot distinguish between  $\Lambda$  and  $\bar{\Lambda}$  produced directly from hadronization of a struck quark and  $\Lambda$  and  $\bar{\Lambda}$  that are decay products. The main contributing decays are  $\Sigma^0 \rightarrow \Lambda\gamma$  and  $\Sigma^* \rightarrow \Lambda\pi$ . Following the procedure adopted by [13, 14] we use the Monte Carlo simulations discussed above to estimate the contributions from all sources. In figure 2 we compare the experimental results with calculations based on two models [11] pertaining to  $\Lambda$  and  $\bar{\Lambda}$  detected in the current fragmentation region. One is the naïve quark model where all baryons are three-quark states with wave functions having zero orbital angular momentum and all the spin of the baryon comes from quark spins. The second is the  $SU(3)_F$  symmetry model where the spin structure of  $SU(3)$  octet hyperons can be deduced from that of the proton [8]. The calculations shown by the curves in figure 2 were done according to the procedures derived in [11] and adapted to the experimental conditions of the present data. The E665 Monte Carlo is used to simulate the contributions from struck quarks and from  $\Sigma^0$  and  $\Sigma^*$  decays. The polarizations were computed with respect to the direction of the virtual-photon spin.

Measurements of  $\Lambda$  polarization at the Z pole [13, 14] show good agreement with calculations in which the spin structure of the  $\Lambda$  was taken from the naïve quark model and the fragmentation calculated using JETSET-based Monte Carlo simulations. This agreement motivated the calculations shown in figure 2 as discussed above [11]. These calculations show a trend of increasing positive polarization with increasing  $x_F$  that seems to be suggested by the data. The statistics and  $x_F$  range of the present data do not allow to confirm this trend more precisely. The large negative value of the measured  $\Lambda$  polarization at  $\langle x_F \rangle = 0.15$  is intriguing. For such low  $x_F$  values the models shown in figure 2 are not very reliable as these models are expected to work better for relatively large  $x_F$ . This result suggests a significant contribution from target fragmentation effects which appear at low and negative  $x_F$  values and favor the  $\Lambda$  over the  $\bar{\Lambda}$  [21]. In anti-neutrino data a large negative  $\Lambda$  polarization has also been observed [22]. Ellis *et al.* [4, 5] have been able to explain this result by assuming that all the sea quark pairs are coupled to a triplet-p state ( $^3P_0$ ) and are polarized oppositely to the valence quark. The authors apply their model to Muon DIS only for the case where the virtual photon is absorbed by a valence quark. In this case, which is not appropriate for the kinematics of the present work, they predict a positive  $\Lambda$  polarization. However, their model can be extended to the case where the virtual photon is absorbed by a sea quark as the kinematics of the present work imply. If we assume that all  $s\bar{s}$  pairs in the sea are coupled to  $^3P_0$ , when a positively polarized photon is absorbed by the negatively polarized member of the pair, the remnant strange quark is likely to be negatively polarized. If the spin of the remnant  $\Lambda$  is determined by that of the remnant strange quark, it will also have a negative polarization. While the actual process may be more complex and these arguments cannot describe it quantitatively, they can indicate a possible source for negative polarization as is actually observed.

In conclusion, we have presented the first results of  $\Lambda$  and  $\bar{\Lambda}$  polarization measured in polarized deep inelastic muon scattering on the nucleon. The results are consistent with the expected trend towards positive polarization with increasing  $x_F$ . A large negative polarization of the  $\Lambda$  at low  $x_F$  is observed suggesting that target fragmentation remains important in this region.

This work was performed at the Fermi National Accelerator Laboratory, which is operated by Universities Research Association, Inc., under contract with the U.S. Dept. of Energy. The work was supported by the U.S Department of Energy, the National Science Foundation (USA), the Bundesministerium für Forschung und Technologie (Germany), the Polish Committee for Scientific Research, the Hungarian Science Foundation and the Israel Science Foundation.

## References

- [1] The CERN SMC collaboration, B. Adeva *et al.*, *Phys. Rev.* **D58**, 112001 (1998).
- [2] The SLAC E143 collaboration, K. Abe *et al.*, *Phys. Rev.* **D58**, 112003 (1998).
- [3] The HERMES collaboration, A. Airapetian *et al.*, *Phys.Lett.* **B442**, 484 (1998).
- [4] J. Ellis, M. Karliner, D.E. Kharzeev and M.G. Sapozhnikov, *Phys. Lett* **B353**, 319 (1995).
- [5] J. Ellis, D. Kharzeev and A. Kotzinian, *Z. Phys.* **C69**, 467 (1996).
- [6] A. Kotzinian, A. Bravar and D. Von Harrach, *Eur. Phys. J.* **C2**, 329 (1998).
- [7] M. Burkardt and R.L. Jaffe, *Phys. Rev. Lett.* **70**, 2537 (1993).
- [8] R.L. Jaffe, *Phys. Rev.* **D54**, R6581 (1996).
- [9] D. DeFlorian *et al.*, *Phys. Rev.* **D57**, 5811 (1998).
- [10] C. Boros and A.W. Thomas hep-ph/9902372 (1999); C. Boros, T.J. Londergan and A.W. Thomas hep-ph/9908260 (1999), to be published.
- [11] D. Ashery and H.J. Lipkin, *Phys. Lett.* in press, hep-ph/9908355.
- [12] M.R. Adams *et al.*, *Z. Phys.* **C61**, 539 (1994).
- [13] The ALEPH collaboration, D. Buskulic *et al.*, *Phys. Lett.* **B374**, 319 (1996).
- [14] The OPAL collaboration, K. Ackerstaff *et al.*, *Eur. Phys. J.* **C2**, 49 (1998).
- [15] M.R. Adams *et al.*, *Nucl. Inst. Meth.* **A291**, 553 (1990).
- [16] G. Ingelman, The Lund Monte Carlo for deep-inelastic lepton-nucleon scattering (1983); T. Sjöstrand, *Comp. Phys. Comm.* **39**, 347 (1986).
- [17] A. Arvidson and B. Badelek, The GAMRAD program, NMC/92/5 (1992).
- [18] R. Brun *et al.* GEANT: Users guide and reference manual, CERN-DD/78/2 (1978).
- [19] M.R. Adams *et al.*, *Z. Phys.* **C74**, 237 (1997).
- [20] Particle Data Group, C. Caso *et al.*, *European Physical Journal* **C3**, 1 (1998).
- [21] M. Arneodo *et al.*, *Phys. Lett.* **145B**, 156 (1984).
- [22] S. Willocq *et al.*, *Z. Phys.* **C53**, 207 (1992)

Table 1: Longitudinal polarizations  $\mathbf{P}_\Lambda^{\text{meas}}$  obtained from straight line fits to  $\cos\theta_{p,\gamma^*}$  distributions of data corrected for detection acceptance and the undiluted polarizations  $\mathbf{P}_\Lambda$ . The signs are with respect to the direction of the spin of the virtual photon. The results are shown for  $\Lambda$  and  $\bar{\Lambda}$  in various  $x_F$  ranges.

	$x_F$ range	$\langle x_F \rangle$	$P_\Lambda^{\text{meas}}$	$\Delta P_{\text{stat}}$	$\Delta P_\Lambda^{\text{meas}}$	$P_\Lambda$	$\Delta P_\Lambda$
$\Lambda$	0. - 0.3	0.15	-0.42	0.14	0.17	-1.2	0.5
$\Lambda$	0.3 - 1.0	0.44	-0.09	0.16	0.19	-0.32	0.7
$\Lambda$	0.1 - 1.0	0.31	-0.23	0.07	0.12	-0.74	0.4
$\bar{\Lambda}$	0. - 0.3	0.15	0.09	0.17	0.20	0.26	0.6
$\bar{\Lambda}$	0.3 - 1.0	0.44	0.31	0.20	0.22	1.1	0.8
$\bar{\Lambda}$	0.1 - 1.0	0.31	0.02	0.13	0.16	0.06	0.5



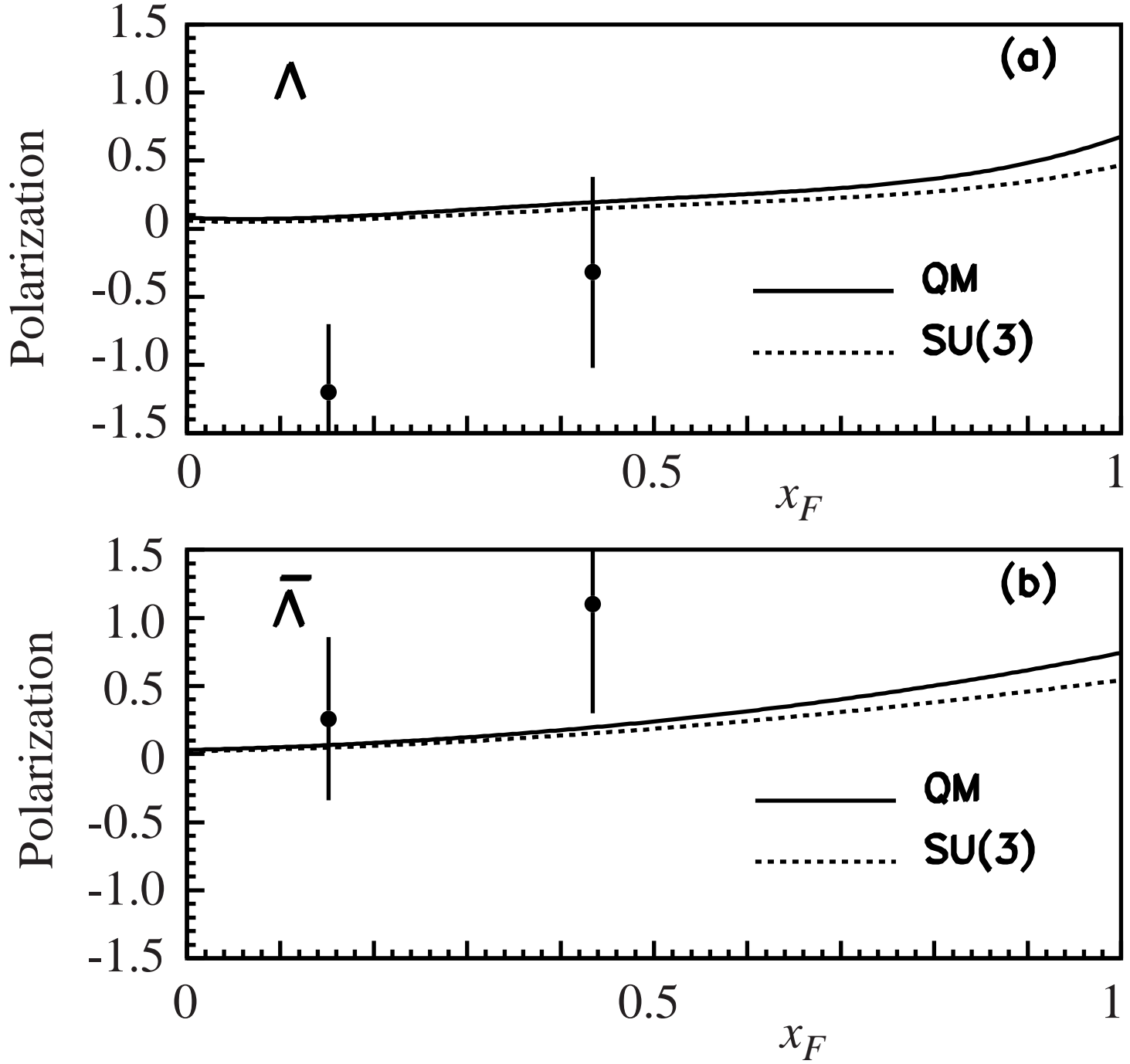


Figure 2: The polarization  $P_\Lambda$  of  $\Lambda$  and  $\bar{\Lambda}$  hyperons. The full circles are for data in the low and high  $x_F$  bins corrected for beam polarization and photon depolarization. The curves are from [11] and show the predictions of the naïve quark model and by assuming SU(3) symmetry.